ACS OMEGA

Open Access

http://pubs.acs.org/journal/acsodf

Article

Design and Synthesis of BODIPY and Its Application in Inhibiting Intestinal Flora

Jinyao Xu,[‖] Hao Huang,[‖] Kewei Wang, Jiatao Zhu, Jiale Zhao, Yingshi Zhao, Jiangtao Yue, Cui Ying, Weijing Tao, Qiang Tong,* Li Quan,* and Jinbing Xie*

Cite This: *ACS Omega* 2024, 9, 44379−44384

Read Online

ACCESS | Metrics & More | Article Recommendations | Supporting Information

ABSTRACT: BODIPY-based photosensitizers were synthesized and tested for antimicrobial photodynamic therapy, revealing structural modifications enhancing the photodynamic therapy (PDT) effects. This research may lead to new PDT strategies for treating bacterial infections, including those resistant to traditional antibiotics, and offers insights into the prevention and treatment of Alzheimer's disease through gut microbiota regulation.

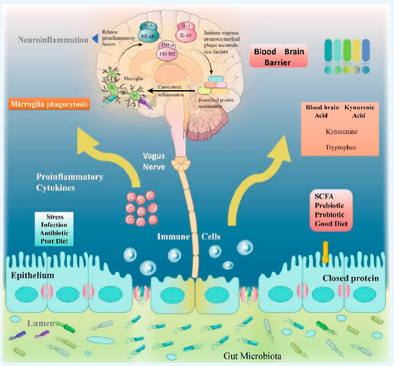

1. INTRODUCTION

Alzheimer's disease (AD) is a neurodegenerative disorder characterized by the degeneration of brain cells.[1−5] The number of microbes in the gut far exceeds the total number of cells in the brain.[6] The study found that certain members of the gut microbiota are capable of producing bacterial amyloid peptides, which may be related to the pathogenesis of AD. *Escherichia coli* (*E. coli*) is the most predominant and abundant bacterium in the gut microbiota, while *Staphylococcus aureus* (S. aureus) is the most pathogenic Gram-positive bacterium. As representative major species, they are often used in various biological and antibacterial experiments. Moreover, these two types of bacteria can produce bacterial amyloid peptides, which can induce neuronal apoptosis and promote the deposition of *Aβ*, thus participating in the occurrence and development of AD.[7,8] In recent years, researchers have proposed the concept of the "microbial-gut-brain axis" from the perspective of intestinal microbes and found that intestinal flora is closely related to AD. The interaction between the "microbial-gut-brain axis" has a significant impact on neurodegenerative diseases and other central nervous system (CNS)-related diseases.[9] Studies on AD at the University of Geneva and Geneva University Hospital further confirm that AD and gut microbiota are linked, and the gut microbiota of AD patients changes dramatically compared to age- and sex-matched controls. For example, the diversity decreases sharply, and the composition is significantly different.[10] Changes in the gut microbiome may affect the onset and progression of AD.[11,12]

Antibacterial photodynamic therapy (APDT) is a non-invasive, clinically recognized, and safe treatment strategy. As an excellent photosensitizer, BODIPY has a promising application in APDT. It exhibits a high absorption coefficient in the visible-light region, high resistance to photobleaching, low dependence on photophysical signals of environmental conditions, small size, and high lipophilicity, thereby promoting the penetration of biofilms. On the other hand, the highly multifunctional nature of the BODIPY parent nucleus provides rich BODIPY chemical properties, making it possible to finely modulate different properties, including key photophysical features.[13−15]

Five BODIPY derivatives, 5MeBDP, 5MeBDP-I, 4MeBDP, 4MeBDP-I, and PhBDP, were synthesized in this study (Figure 1). The *π*-conjugation system of BODIPY can be altered by suffixing two iodine atoms at the 2 and 6 positions of the "BDP

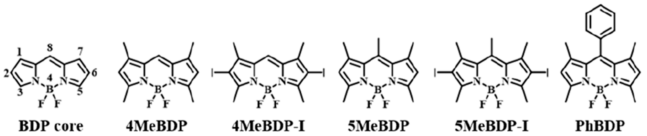

Figure 1. BODIPY derivatives BDPs: BDP core, 5MeBDP, 5MeBDP-I, 4MeBDP, 4MeBDP-I, and PhBDP.

Received: June 11, 2024
Revised: September 12, 2024
Accepted: September 17, 2024
Published: October 25, 2024

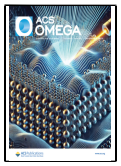

core" (Figure 1) and introducing a benzene ring at the 8 position to red-shift its maximum absorption peak. The use of structurally active rotational energy levels increases the likelihood of nonradiative transitions, thus significantly increasing the level of $^1O_2$ production and yielding BODIPY photosensitizers (PSs) with good optical properties. In vitro antimicrobial assays showed that all five BODIPY derivatives were effective in killing bacteria under laser irradiation (λ = 545 nm, 100 mW).

The most common method involves introducing heavy atoms such as iodine into its structure, which can lead to a decrease in fluorescence intensity, a shortened fluorescence lifetime, an enhancement of intersystem transition to the T1 state, and stability of the T1 state.[16,21] Heavy atoms at positions 2 and 6 of BODIPY resulted in absorption and fluorescence shifts, greatly increased the oxygen production, and significantly reduced the number of S. aureus.[17−20]

Here, the development of new PSs based on BODIPY dyes is discussed, which are used in photodynamic therapy (PDT). The research aims to overcome limitations of conventional PSs by improving their photodynamic activity, $^1O_2$ (singlet oxygen) generation efficiency, and solubility. The "BDP core" of BODIPY is modified by introducing iodine atoms and altering the conjugation system to enhance its properties.

Iodine introduction: heavy atomic iodine at positions 2 and 6 of the "BDP core" increases intersystem migration possibilities, $^1O_2$ production, and photodynamic activity; conjugation system extension: by connecting a benzene ring at the 8 site of the parent nucleus, the conjugation system is changed, leading to a red-shift in the maximum absorption peak to the phototherapeutic window, allowing the use of visible light for photodynamic effects.

2. EXPERIMENTAL PART

2.1. Materials and Instruments. Mouse epithelial cells, BV-2 cell line, *S. aureus* and *E. coli* (ATCC); modified Eagle medium DMEM and fetal bovine serum (Gibco Co.); PBS buffer, 4% paraformaldehyde, glutaraldehyde, 1,3-bis(4-phenylene)vinylbenzofuran (DPBF), CCK-8 rhodamine 123, DAPI staining solution, and penicillin/streptomycin (Biosharp Co.); soybean peptone, agar, yeast dipping powder, sodium chloride (Qingdao Haibo Biotechnology Co., Ltd.); the rest of the experimental materials were provided by Sigma-Aldrich Chemical Co. $CDCl_3$ was used as the solvent. UV/vis spectra were recorded on a UV-2600 spectrophotometer at room temperature. Fluorescence spectra were recorded on an F-7000 spectrophotometer. A 545 nm laser was used as the light source, and the laser output power was controlled by a fiber-coupled laser system (Changchun New Industry Optoelectronics). Scanning electron microscopy observation was performed using a Quanta 250 FEG field emission scanning electron microscope (Keenshine, Japan). A laser particle size analyzer (Malvern) was used. An Epoch2 microplate spectrophotometer was used in CCK-8 determination. CarlZeissA2 inverted fluorescence microscope (Zeiss, Germany) was used for evaluation of fluorescence imaging.

2.2. Compound Synthesis. Details of the synthesis, ^{1}HNMR, basic fluorescence spectra, and colors of the synthesized products of 5MeBDP, 5MeBDP-I, 4MeBDP, 4MeBDP-I, and PhBDP compounds are described in the Supporting Information.

2.3. Charge Distribution of BODIPY. The Gaussian 09w quantum chemistry package was employed and optimally tuned at the B3LYP/6-311G* and LANL2DZ basis group levels using quantum chemical microdensity flood theory (DFT) calculations, and molecular orbital images were drawn using Molden 4.2.

2.4. In Vitro Single-Linear Oxygen Determination. For a detailed program, see Supporting Information.

2.5. Minimum Inhibitory Concentration. The BODIPY PSs solution was diluted in a 96-well plate using a logarithmic gradient of TSB; 100 μL of a bacterial suspension at a concentration of 5×10^5 bacteria/mL was added to each well; and the wells were incubated for 30 min on a shaking bed under laser irradiation at 37 °C. Absorbance at 600 nm was calculated for each well using a microtiter plate spectrophotometer.

2.6. Bacterial Growth Curve Determination. S. aureus and *E. coli* (1×10^8 CFU/mL) were mixed with PBS, DMSO, ETOH, and BDP. The mixture was treated with green light (30 min) or without green light, and then incubated at 37 °C. 600 nm absorbance of each well was calculated by the microplate spectrophotometer.

2.7. In Vivo Colony Counting Method. S. aureus and *E. coli* solutions (10^4 CFU/mL) were first mixed with PBS, DMSO, EtOH, and BODIPY PSs. Mixed solutions were irradiated with or without a 545 nm laser at a light intensity of 100 mW for 30 min. The mixtures were subsequently coated on LB plates and incubated at 37 °C for 24 h. Pictures were taken, and the survival rates of the bacteria in the different treatment groups were calculated.

2.8. CCK-8 Assay to Analyze the Cytotoxicity of the Material. The effect of BODIPY on the survival of mouse endothelial cells and microglia BV-2 was verified using the research-disclosed CCK-8 method to analyze the cytotoxicity of the material, which has been described in detail in the Supporting Information.

2.9. Hemolytic Performance Study of BODIPY. After centrifugation at 1500r, the lowest layer of erythrocytes in the blood was taken for hemolysis study. Red blood cells at a concentration of 2% were diluted with PBS along with different concentrations of BODIPY, and 1 mL of diluted blood was added to each well of a 24-well plate, followed by 1 mL of different concentrations of BODIPY PSs solution. The positive control group included distilled water and 2% red blood cells; the negative control group included PBS solution and 2% red blood cells; and the hemolysis was photographed and observed. The mixed solution (1 mL per well) was centrifuged at 1500 rpm for 5 min, and then 100 μL of the supernatant was placed in a 96-well plate.

2.10. Statistical Analysis. All experimental data were statistically analyzed using one-way ANOVA, and the process of processing the experimental data is described in detail in the Supporting Information.

3. RESULTS AND DISCUSSION

3.1. Design, Synthesis, and Characterization of BODIPY Photosensitizers. Synthetic routes for 5MeBDP, 5MeBDP-I, 4MeBDP, 4MeBDP-I, and PhBDP are detailed, involving several chemical reactions, including condensation, substitution, and oxidation steps (Figure S1). The emission peaks of ten BODIPY PSs in different solvents (DMSO and EtOH) showed a red shift after modification, indicating increased conjugation and potential for improved photodynamic performance (Figure S2). The absorbance of 5MeBDP-I showed a significant red shift after iodine

https://doi.org/10.1021/acsomega.4c04882
ACS Omega 2024, 9, 44379−44384

modification, which may be due to increased spin−orbit coupling and an ISC (intersystem crossing) probability leap from S1 (singlet excited state) to T1 (triplet excited state). Theoretical calculations using the Gaussian 09w program and TDDFT/B3LYP/6-311G* and LANL2DZ basis sets showed clear charge transfer from the methyl substituent and iodine atom to the "BDP core", indicating a favorable photoinduced electron transfer process (Figure 2). Overall, the research

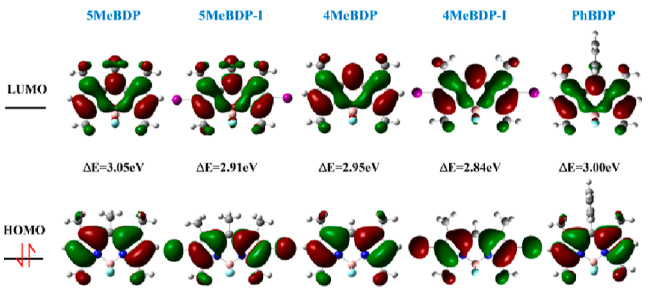

Figure 2. Front-line orbital energy level diagram of BODIPY PSs, Δ*E*: energy polarity different.

appears to be focused on improving PDT efficacy by modifying the structure of BODIPY PSs to enhance their photodynamic properties, which could potentially lead to more effective treatments in the future.

The experimental results described in this passage involve the evaluation of ten BODIPY-based PSs mixed with diphenylborinate (DPBF) and irradiated with a laser for a specific duration (210 s) (Figure S3). The decrease in DPBF light absorption values after treatment with the BODIPY PSs indicates the extent of DPBF degradation, which is used as a proxy for the $^1O_2$ generation capacity of the PSs. The order of the $^1O_2$ generation capacity based on DPBF degradation is as follows: PhBDP/EtOH > 5MeBDP-I/EtOH > 4MeBDP-I/EtOH > 4MeBDP/EtOH > 5MeBDP/EtOH > PhBDP/DMSO > 5MeBDP/DMSO > 4MeBDP/DMSO > 5MeBDP-I/DMSO > 4MeBDP-I/DMSO. The rate ratio of $^1O_2$ production is approximately 0.74:0.46:0.67:0.54:0.26:0.88:0.94:0.83:1:0.57 (Figure 3).

The presence of PSs causes oxygen in the monoclinic state to react with DMSO, forming dimethyl sulfone, which reduces the $^1O_2$ content. This results in weaker $^1O_2$ production for BODIPY dissolved in DMSO compared to BODIPY dissolved in EtOH. Under green light irradiation (λ = 545 nm, 100 mW), the order of $^1O_2$ production capacity for EtOH-solubilized BODIPYs is PhBDP> 5MeBDP-I> 4MeBDP-I> 4MeBDP> 5MeBDP. The absorbance of DPBF at 415 nm gradually levels off after a rapid decrease in the experimental group, suggesting that the BODIPY PSs can continuously produce $^1O_2$ under light conditions and overcome intramolecular charge transfer competition within the first 90 s. The introduction of double iodine atoms at the 2 and 6 positions and a benzene ring at the 8 position significantly reduces DPBF absorbance at 415 nm, indicating that these modifications can greatly enhance the photodynamic activity of BODIPY and promote $^1O_2$ production. Based on these results, all of these BODIPY PSs tested have the potential to generate $^1O_2$ and are considered excellent candidates for advanced photodynamic therapy applications as photosensitizers.

3.2. Photodynamic Antibacterial Activity of BODIPY Photosensitizers. Minimum Inhibitory Concentration (MIC) is a measure of the effectiveness of an antimicrobial agent against a specific microorganism. It is the lowest concentration of the agent that inhibits the visible growth of the microorganism. In this context, the MIC values reported for the BODIPY-based PSs indicate the concentration of PS required to inhibit the growth of the bacteria. In the absence of light, the MIC values for 5MeBDP, 4MeBDP-I, and PhBDP against both Gram-positive and Gram-negative bacteria were greater than 2.5 μg/mL (Figure S5). This means that in the dark these PSs were not effective in inhibiting bacterial growth at the tested concentrations. However, when light was available, the MIC values for 5MeBDP-I diluted with EtOH against Gram-negative bacteria and for 4MeBDP-I and PhBDP against Gram-positive and Gram-negative bacteria were lower, ranging from 1.25 to 2.5 μg/mL. This significant reduction in MIC values under light irradiation suggests that the introduction of a double iodine substitution and the presence of a benzene ring in the BODIPY structure enhance the antibacterial activity of the PSs when they are activated by light. The enhanced activity likely results from the production of singlet oxygen ($^1O_2$) upon light activation, which can cause damage to essential cellular components such as phospholipids, proteins, and nucleic acids. This damage impairs the function of the bacteria and can lead to their death.

For Gram-positive bacteria, the APDT (Photodynamic Therapy) effect of the BODIPY PSs was able to induce $^1O_2$ production, resulting in significant damage and death. However, for Gram-negative bacteria, the change in the MIC values before and after light exposure of the BODIPY PSs was

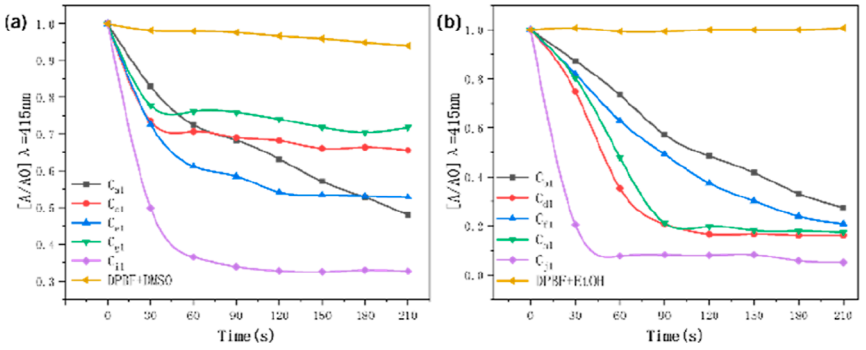

Figure 3. Comparison of $^1O_2$ production rates of 5MeBDP, 5MeBDP-I, 4MeBDP, 4MeBDP-I, and PhBDP (0.01 mg/mL). 5MeBDP, 5MeBDP-I, 4MeBDP, 4MeBDP-I, and PhBDP with DMSO as solvent are denoted as (a) C_{a1}, C_{c1}, C_{e1}, C_{g1}, and C_{i1} and with EtOH as the solvent are denoted as (b) C_{b1}, C_{d1}, C_{f1}, C_{h1}, and C_{j1}.

https://doi.org/10.1021/acsomega.4c04882
ACS Omega 2024, 9, 44379−44384

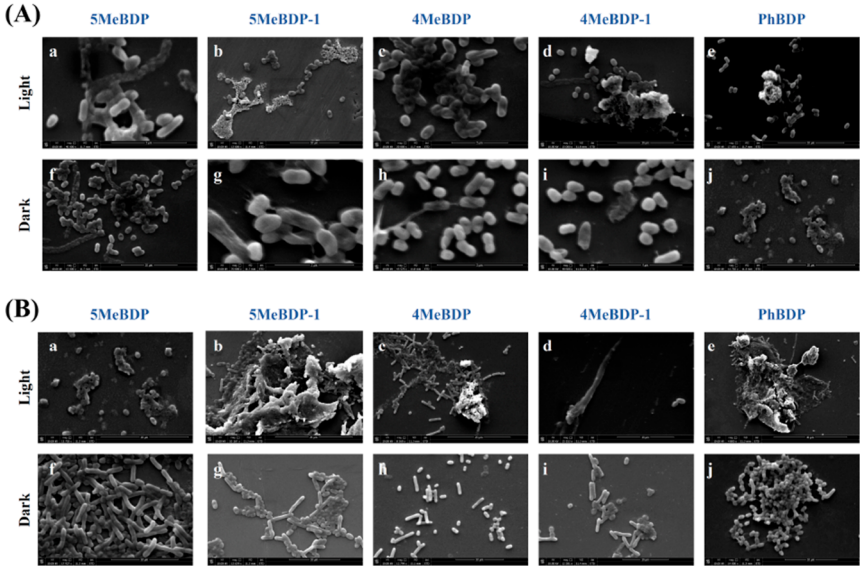

Figure 4. Scanning electron micrographs of (A) S. aureus and (B) *E. coli*. 5MeBDP, 5MeBDP-I, 4MeBDP, 4MeBDP-I, and PhBDP light treatments (a, b, c, d, e) and nonlight treatments (f, g, h, i, j).

minimal. This could be due to the more complex and compact cell wall structure of Gram-negative bacteria, which includes an additional outer membrane. This outer membrane acts as a strong defense barrier and may prevent the PSs from reaching their target within the bacterial cell, thereby reducing their effectiveness. Additionally, the outer membrane may adsorb or degrade the PSs, further protecting the bacteria from damage. In summary, the introduced structural modifications in the BODIPY PSs and the activation by light can significantly enhance their antibacterial activity against Gram-positive bacteria. However, the presence of an outer membrane in Gram-negative bacteria presents a challenge, as it limits the efficacy of the PSs. Further research may be needed to develop strategies to overcome this barrier and improve the antibacterial activity of these PSs against Gram-negative bacteria.

A detailed analysis of the antibacterial activity of various BODIPY-based PSs against *S. aureus* and *E. coli* is presented, comparing their effects in the presence and absence of light. The bacterial survival rate was calculated using UV spectrophotometry to determine the effectiveness of the PSs in reducing bacterial growth (Figure S4). The survival rate is expressed as a percentage of the optical density (OD) at 600 nm of the treated bacteria (T_{OD600}) compared to the OD of the control bacteria (C_{OD600}). The bacterial survival rate was calculated as follows

$$\textbf{Bacterial Survival}(\%) = \frac{\mathbf{T_{OD600}}}{\mathbf{C_{OD600}}} \times \mathbf{100}\%$$

The results showed that the untreated bacterial survival rates for both S. aureus and *E. coli* were above 70% under light exposure. 5MeBDP and 4MeBDP solubilized in EtOH showed no significant antibacterial effect against S. aureus in the dark. Other BODIPY PSs reduced the bacterial survival rates by about 7−22%. This effect may be due to irregular light penetration during the experimental process, leading to the production of a small amount of singlet oxygen. Light exposure significantly reduced bacterial survival rates, with survival rates decreasing by 15−50%. BODIPY showed a high inhibitory effect on S. aureus, and DMSO-solubilized 4MeBDP had reduced activity against Gram-negative bacteria compared with other BODIPY PSs, possibly due to solubility issues. The bacterial growth curves indicated that both Gram-positive and Gram-negative bacteria experienced a delayed growth period and a logarithmic growth period. S. aureus and *E. coli* reached their highest growth rates after about 18 h and then entered a slow growth phase, with *E. coli* showing the best growth activity under regular inoculation.

To improve the antibacterial activity against Gram-negative bacteria, two approaches were suggested: using specific compounds or incorporating positively charged groups into the PSs to enhance their bactericidal properties.[22,23] The growth curves of BODIPY PSs solubilized in DMSO showed trends similar to those of the control in the absence of light, while those solubilized in EtOH showed inhibition of both bacteria. Laser irradiation for 30 min before incubation resulted in the most drastic bacterial growth inhibition at 36 h after incubation, with EtOH-solubilized PhBDP showing almost complete inhibition of both bacteria, regardless of light exposure. The solvent used (DMSO or EtOH) affected the photodynamic bactericidal effect of the BODIPY PSs. EtOH had less fluorescence burst effect on BODIPY compared to DMSO, leading to better sterilization performance of BODIPY PSs dissolved in EtOH (Figure S6). In summary, the studies indicate that BODIPY PSs have significant antibacterial efficacy under light activation with specific PSs showing higher inhibitory effects on S. aureus. The solubility of the PSs in different solvents and their ability to produce $^1O_2$ play crucial roles in their antibacterial activity, particularly against Gram-negative bacteria. Further research could focus on optimizing the structure of BODIPY PSs to enhance their effectiveness against Gram-negative bacteria and improve their solubility in solvents like EtOH.

DNA and RNA in the cytoplasm of bacteria absorb UV light at 260 nm. The degree of absorption can be used to track the release of cytoplasmic components from bacterial cells (Figure S7).[24] It was found that light-activated BODIPY-treated bacteria had higher absorption at 260 nm, indicating damage to the cell membrane. Scanning electron microscopy images showed that bacterial cells treated with BODIPY and exposed

https://doi.org/10.1021/acsomega.4c04882
ACS Omega 2024, 9, 44379−44384

to green laser irradiation exhibited structural changes such as folds, collapses, and depressions on their surfaces with the edges of colonies becoming blurred. The $^1O_2$ produced by light acted on lipids through oxidative reactions, damaging the bacterial cell membrane and leading to bacterial death. This reveals the photodynamic antibacterial mechanism of BODIPY (Figure 4).

Using the CCK-8 reduction method, the study evaluated the inhibitory effect of BODIPY on endothelial cell growth. PhBDP did not show significant cytostatic effects in the dark at concentrations ranging from 0.625 to 10 μg/mL. However, under green laser irradiation, significant cytotoxicity was observed, suggesting that the photodynamic effects of PhBDP can lead to cell death (Figure S8a).

Hemolysis assay evaluated the potential hemolytic activity of BODIPY when mixed with red blood cells (Figure S8b). The results indicated that BODIPY can lyse hemoglobin and destroy erythrocytes, but the hemolysis rate was relatively low (10% to 33%), which is considered acceptable for certain biomedical applications.[25]

Overall, the findings suggest that BODIPY PSs have potential applications as biomarkers for in vitro and in vivo studies, particularly in the context of photodynamic therapy for bacteria and possibly other pathogens. However, further research is needed to evaluate their broader cytotoxic effects and compatibility with biological systems.

4. CONCLUSIONS

The thesis examines the synthesis and antimicrobial properties of five BODIPY-based PSs: 5MeBDP, 5MeBDP-I, 4MeBDP, 4MeBDP-I, and PhBDP. The research primarily focuses on the antimicrobial activity of BODIPY and investigates how modifications to the BODIPY structure can enhance its PDT effects. Here is a breakdown of the key points:

BODIPY as the master core: BODIPY is a fluorescent dye that serves as the core structure for the synthesis of the PSs. Its properties, such as the ability to absorb light and generate reactive oxygen species (ROS) like $^1O_2$, make it suitable for PDT, which can lead to the killing of microorganisms.

Antimicrobial properties under light activation: the study aimed to assess the antimicrobial capabilities of the five compounds when activated by light. Light activation triggers the release of ROS, which damages microbial cells and results in their death.

Structural modifications for the enhanced PDT effects: the research investigated how the introduction of different chemical groups or modifications to the BODIPY structure affected the PDT effects. In particular, the introduction of a benzene ring at position 8 of the "BDP core" was noted as a modification that could potentially improve PDT effects. This alteration might enhance the π (pi) system of the molecule, leading to improved light absorption and increased efficiency in ROS generation.

Mechanisms of action: the thesis explored the specific mechanisms by which these BODIPY PSs caused the death of bacteria or other microorganisms. These mechanisms could include direct damage to cell membranes by ROS, the induction of DNA damage, or the disruption of essential cellular processes.

PDT: PDT is a promising noninvasive treatment for various diseases, including cancer, infections, and certain skin conditions. It utilizes light-activated drugs to generate ROS that selectively kill cancer cells or pathogens while preserving normal cells.

By synthesizing and testing these BODIPY PSs, the thesis contributes to the development of new PDT options for antimicrobial applications. The findings could pave the way for the design of more effective photosensitizers for PDT, which is essential for the development of new therapies for bacterial infections, particularly those that are resistant to conventional antibiotics.

■ ASSOCIATED CONTENT

Supporting Information

The Supporting Information is available free of charge at https://pubs.acs.org/doi/10.1021/acsomega.4c04882.

Additional experimental details and materials and methods for all compounds, including photographs of experimental setups (PDF)

■ AUTHOR INFORMATION

Corresponding Authors

Qiang Tong − *Department of Neurology, The Affiliated Huaian First People's Hospital of Nanjing Medical University, Huaian, Jiangsu 223001, China*; Email: dr_tongqiang@126.com

Li Quan − *Jiangsu Provincial Engineering Research Center for Biomedical Materials and Advanced Medical Devices, Faculty of Mechanical and Material Engineering, Huaiyin Institute of Technology, Huaian, Jiangsu 223003, China*; orcid.org/0000-0003-4776-8300; Email: quanli99@126.com

Jinbing Xie − *Department of Radiology, Zhongda Hospital, Nurturing Center of Jiangsu Province for State Laboratory of AI Imaging & Interventional Radiology, School of Medicine, Southeast University, Nanjing, Jiangsu 210009, China*; orcid.org/0000-0002-6071-0878; Email: xiejb@seu.edu.cn

Authors

Jinyao Xu − *Jiangsu Provincial Engineering Research Center for Biomedical Materials and Advanced Medical Devices, Faculty of Mechanical and Material Engineering, Huaiyin Institute of Technology, Huaian, Jiangsu 223003, China*

Hao Huang − *Jiangsu Provincial Engineering Research Center for Biomedical Materials and Advanced Medical Devices, Faculty of Mechanical and Material Engineering, Huaiyin Institute of Technology, Huaian, Jiangsu 223003, China*

Kewei Wang − *Jiangsu Provincial Engineering Research Center for Biomedical Materials and Advanced Medical Devices, Faculty of Mechanical and Material Engineering, Huaiyin Institute of Technology, Huaian, Jiangsu 223003, China*

Jiatao Zhu − *Jiangsu Provincial Engineering Research Center for Biomedical Materials and Advanced Medical Devices, Faculty of Mechanical and Material Engineering, Huaiyin Institute of Technology, Huaian, Jiangsu 223003, China*

Jiale Zhao − *Jiangsu Provincial Engineering Research Center for Biomedical Materials and Advanced Medical Devices, Faculty of Mechanical and Material Engineering, Huaiyin Institute of Technology, Huaian, Jiangsu 223003, China*

Yingshi Zhao − *Jiangsu Provincial Engineering Research Center for Biomedical Materials and Advanced Medical Devices, Faculty of Mechanical and Material Engineering, Huaiyin Institute of Technology, Huaian, Jiangsu 223003, China*

https://doi.org/10.1021/acsomega.4c04882
ACS Omega 2024, 9, 44379−44384

Jiangtao Yue − *Jiangsu Provincial Engineering Research Center for Biomedical Materials and Advanced Medical Devices, Faculty of Mechanical and Material Engineering, Huaiyin Institute of Technology, Huaian, Jiangsu 223003, China*
Cui Ying − *Department of Radiology, Zhongda Hospital, Nurturing Center of Jiangsu Province for State Laboratory of AI Imaging & Interventional Radiology, School of Medicine, Southeast University, Nanjing, Jiangsu 210009, China*
Weijing Tao − *Department of Neurology, The Affiliated Huaian First People's Hospital of Nanjing Medical University, Huaian, Jiangsu 223001, China*

Complete contact information is available at: https://pubs.acs.org/10.1021/acsomega.4c04882

Author Contributions

‖J.Y. Xu and H. Huang contributed equally to this paper.

Notes

The authors declare no competing financial interest.

■ ACKNOWLEDGMENTS

This work was supported by grants from the start-up fund of Huaiyin Institute of Technology (Z421A17641), Science Foundation of Jiangsu Provincial Department of Education (22KJA430010), the National Natural Science Foundation of China (51803068), and the Jiangsu Qing Lan project.

■ REFERENCES

(1) Mawuenyega, K. G.; Sigurdson, W.; Ovod, V.; Munsell, L.; Kasten, T.; Morris, J. C.; Yarasheski, K. E.; Bateman, R. J. Decreased Clearance of CNS β-Amyloid in Alzheimer's Disease. *Science* **2010**, *330* (6012), 1774.
(2) Honjo, K.; Van, R. R.; Verhoeff, N. P. Alzheimer's disease and infection: do infectious agents contribute to progression of Alzheimer's disease? *Alzheimers Dement.* **2009**, *5* (4), 348−360.
(3) Ganz, T. F. N.; Ben-Hur, T. When the infectious environment meets the AD brain. *Mol. Neurodegener.* **2022**, *17* (1), 53.
(4) Rutsch, A.; Kantsjö, J. B.; Ronchi, F. The Gut-Brain Axis: How Microbiota and Host Inflammasome Influence Brain Physiology and Pathology. *Front. Immunol.* **2020**, *11*, 604179.
(5) Martin, C. R.; Osadchiy, V.; Kalani, A.; Mayer, E. A. The Brain-Gut-Microbiome Axis. *Cell. Mol. Gastroenter.* **2018**, *6* (2), 133−148.
(6) Thursby, E.; Juge, N. Introduction to the human gut microbiota. *Biochem. J.* **2017**, *474* (11), 1823−1836.
(7) Gao, J.; Jiang, Q.; Luo, Z.; Sun, X.; Dai, X. Cultivation and identification of normal intestinal bacteria in tree shrews and their drug sensitivity test. *Chin. J. Comp. Med.* **2009**, *19* (12), 24−26.
(8) Wang, J.; Xia, J.; Zhao, N.; Gao, L.; Xu, B. Exercise improves inflammatory pathology in Alzheimer's disease by modulating the gut flora-gut-brain axis immune pathway. *Life Sci.* **2022**, *34*, 599−607.
(9) Perry, V. H.; Cunningham, C.; Holmes, C. Systemic infections and inflammation affect chronic neurodegeneration. *Nat. Rev. Immunol.* **2007**, *7* (2), 161−167.
(10) Jiang, C.; Li, G.; Huang, P.; Liu, Z.; Zhao, B. The Gut Microbiota and Alzheimer's Disease. *J. Alzheimers Dis.* **2017**, *58* (1), 1−15.
(11) Cattaneo, A.; Cattane, N.; Galluzzi, S.; Provasi, S.; Lopizzo, N.; Festari, C.; Ferrari, C.; Guerra, U. P.; Paghera, B.; Muscio, C.; et al. Association of brain amyloidosis with pro-inflammatory gut bacterial taxa and peripheral inflammation markers in cognitively impaired elderly. *Neurobiol. Aging* **2017**, *49*, 60−68.
(12) Minter, M. R.; Zhang, C.; Leone, V.; Ringus, D. L.; Zhang, X.; Oyler-Castrillo, P.; Musch, M. W.; Liao, F.; Ward, J. F.; Holtzman, D. M.; Chang, E. B.; Tanzi, R. E.; Sisodia, S. S. Antibiotic-induced perturbations in gut microbial diversity influences neuro-inflammation and amyloidosis in a murine model of Alzheimer's disease. *Sci. Rep.* **2016**, *6* (1), 30028.
(13) Wang, Z.; Dong, K.; Liu, Z.; Zhang, Y.; Chen, Z.; Sun, H.; Ren, J.; Qu, X. Activation of biologically relevant levels of reactive oxygen species by Au/g-C(3)N(4) hybrid nanozyme for bacteria killing and wound disinfection. *Biomaterials* **2017**, *113*, 145−157.
(14) Ji, H.; Sun, H.; Qu, X. Antibacterial applications of graphene-based nanomaterials: Recent achievements and challenges. *Adv. Drug Delivery Rev.* **2016**, *105*, 176−189.
(15) Wang, J.; Boens, N.; Jiao, L.; Hao, E. Aromatic [b]-fused BODIPY dyes as promising near-infrared dyes. *Org. Biomol. Chem.* **2020**, *18* (22), 4135−4156.
(16) Yogo, T.; Urano, Y.; Ishitsuka, Y.; Maniwa, F.; Nagano, T. Highly efficient and photostable photosensitizer based on BODIPY chromophore. *J. Am. Chem. Soc.* **2005**, *127* (35), 12162−12163.
(17) Turksoy, A.; Yildiz, D.; Akkaya, E. U. Photosensitization and controlled photosensitization with BODIPY dyes. *Coord. Chem. Rev.* **2019**, *379*, 47−64.
(18) Kue, C. S.; Kamkaew, A.; Voon, S. H.; Kiew, L. V.; Chung, L. Y.; Burgess, K.; Lee, H. B. Tropomyosin Receptor Kinase C Targeted Delivery of a Peptidomimetic Ligand-Photosensitizer Conjugate Induces Antitumor Immune Responses Following Photodynamic Therapy. *Sci. Rep.* **2016**, *6* (1), 37209.
(19) Ge, Y.; O'Shea, D. F. Azadipyrromethenes: from traditional dye chemistry to leading edge applications. *Chem. Soc. Rev.* **2016**, *45* (14), 3846−3864.
(20) Peveler, W. J.; Noimark, S.; Al-Azawi, H.; Hwang, G. B.; Crick, C. R.; Allan, E.; Edel, J. B.; Ivanov, A. P.; MacRobert, A. J.; Parkin, I. P. Covalently Attached Antimicrobial Surfaces Using BODIPY: Improving Efficiency and Effectiveness. *ACS Appl. Mater. Interfaces* **2018**, *10* (1), 98−104.
(21) Durantini, A. M.; Greene, L. E.; Lincoln, R.; Martínez, S. R.; Cosa, G. Reactive Oxygen Species Mediated Activation of a Dormant Singlet Oxygen Photosensitizer: From Autocatalytic Singlet Oxygen Amplification to Chemicontrolled Photodynamic Therapy. *J. Am. Chem. Soc.* **2016**, *138* (4), 1215−1225.
(22) Castriciano, M. A.; Zagami, R.; Casaletto, M. P.; Martel, B.; Trapani, M.; Romeo, A.; Villari, V.; Sciortino, M. T.; Grasso, L.; Guglielmino, S.; et al. Poly(carboxylic acid)-Cyclodextrin/Anionic Porphyrin Finished Fabrics as Photosensitizer Releasers for Antimicrobial Photodynamic Therapy. *Biomacromolecules* **2017**, *18* (4), 1134−1144.
(23) Chen, L. L.; Zheng, M. L.; Zheng, Y. C.; Jin, F.; Chai, Q. Q.; Zhao, Y. Y.; Meng, X. W.; Liu, Y. H.; Duan, X. M. Laser-Induced Antibacterial Activity of Novel Symmetric Carbazole-Based Ethynylpyridine Photosensitizers. *ACS Omega* **2018**, *3* (4), 3737−3743.
(24) Meng, X.; Li, D.; Zhou, D.; Wang, D.; Liu, Q.; Fan, S. Chemical composition, antibacterial activity and related mechanism of the essential oil from the leaves of Juniperus rigida Sieb. et Zucc against Klebsiella pneumoniae. *J. Ethnopharmacol.* **2016**, *194*, 698−705.
(25) Zhang, W.; Liu, F. Effect of Polylysine on Blood Clotting, and Red Blood Cell Morphology, Aggregation and Hemolysis. *J. Nanosci. Nanotechnol.* **2017**, *17* (1), 251−255.